

## This article is featured in the Special Issue on TRIBOLOGY

### Guest editors:

Ezequiel Alberto GALLARDO HERNÁNDEZ | Instituto Politecnico Nacional

Manuel VITE TORRES | Instituto Politecnico Nacional

Nelson Federico GARZA MONTES DE OCA | Universidad Autónoma de Nuevo León

César SEDANO DE LA ROSA | Universidad de Guadalajara

Erosive wear of AISI S1 and AISI H13 steels caused by spherical and angular particles

*Desgaste erosivo de los aceros AISI S1 y AISI H13 causado por partículas esféricas y angulares*

Juan Rodrigo **Laguna Camacho**  
Universidad Veracruzana | MÉXICO

Aldo Santos **Calderon Loredo**  
Universidad Veracruzana | MÉXICO

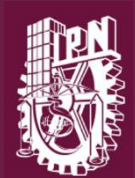
Víctor **Velázquez Martínez**  
Universidad Veracruzana | MÉXICO

Javier **Calderón Sánchez**  
Instituto Politécnico Nacional | MÉXICO

Héctor Daniel **López Calderón**  
Universidad Veracruzana | MÉXICO

<https://cientifica.site>

Recibido 15/04/2026, aceptado 25/05/2026.



## Erosive wear of AISI S1 and AISI H13 steels caused by spherical and angular particles

Desgaste erosivo de los aceros AISI S1 y AISI H13 causado por partículas esféricas y angulares

Juan Rodrigo **Laguna Camacho**<sup>1\*</sup>  
Aldo Santos **Calderon Loredo**<sup>2</sup>  
Víctor **Velázquez Martínez**<sup>3</sup>  
Javier **Calderón Sánchez**<sup>4</sup>  
Héctor Daniel **López Calderón**<sup>5</sup>

Universidad Veracruzana, Facultad de Ingeniería Mecánica y Eléctrica,  
Poza Rica de Hidalgo, MÉXICO

<sup>1</sup> ORCID: 0000-0001-5989-3972 / [jlaguna@uv.mx](mailto:jlaguna@uv.mx)\*

<sup>2</sup> ORCID: 0000-0001-5343-8346 / [vivelazquez@uv.mx](mailto:vivelazquez@uv.mx)

<sup>3</sup> ORCID: 0000-0002-1382-1081 / [jacalderon@uv.mx](mailto:jacalderon@uv.mx)

Instituto Politécnico Nacional, Escuela Superior de Ingeniería Mecánica y Eléctrica,  
Ciudad de México, MÉXICO

<sup>4</sup> ORCID: 0009-0006-4263-9496 / [aldo2900@hotmail.com](mailto:aldo2900@hotmail.com)

Universidad Veracruzana, Facultad de Biología,  
Xalapa, MÉXICO

<sup>5</sup> ORCID: 0000-0001-6324-537X / [hectolopez@uv.mx](mailto:hectolopez@uv.mx)

<https://cientifica.site>

Recibido 15/04/2026, aceptado 25/05/2026.



## Abstract

In this work, an analysis of erosive wear was carried out on hot-work tool steels, AISI S1 (non-deformable steel with high chromium content) and AISI H13 (steel with high chromium, molybdenum, and vanadium content) subjected to the impact of alumina spherical particles ( $\text{Al}_2\text{O}_3$ ) and silicon carbide angular particles (SiC), to understand their behaviour and performance under different particle shapes. An erosion rig based on the ASTM G76-95 standard was used to perform the testing. Tests were carried out using different impact angles,  $30^\circ$ ,  $45^\circ$ ,  $60^\circ$  and  $90^\circ$ , with a particle velocity of  $30 \pm 2$  m/s and a particle flux of 63 g/min. Characterization techniques such as hardness tests and optical microscopy was used to know the morphology of the abrasive particles and identify the wear mechanisms. The erosion rates showed that AISI S1 steel exhibited higher erosion resistance than AISI H13 steel after the consistent impingement of abrasive particles. In addition, SiC particles inflicted higher erosion damage on surfaces than  $\text{Al}_2\text{O}_3$  grits.

**Index terms:** erosive wear, AISI S1 steel, AISI H13, particle shape, erosion rates.

## 2

## Resumen

En este trabajo, se realizó un análisis del desgaste erosivo en aceros para herramientas de trabajo en caliente, AISI S1 (acero no deformable con alto contenido de cromo) y AISI H13 (acero con alto contenido de cromo, molibdeno y vanadio), sometidos al impacto de partículas esféricas de alúmina ( $\text{Al}_2\text{O}_3$ ) y angulares de carburo de silicio (SiC), para comprender su comportamiento y rendimiento bajo diferentes formas de partículas. Se utilizó un equipo de pruebas de erosión basado en la norma ASTM G76-95 para realizar las pruebas. Estas se llevaron a cabo utilizando diferentes ángulos de impacto,  $30^\circ$ ,  $45^\circ$ ,  $60^\circ$  y  $90^\circ$ , con una velocidad de partícula de  $30 \pm 2$  m/s y un flujo de partícula de 63 g/min. Se utilizaron técnicas de caracterización como pruebas de dureza y microscopía óptica para conocer la morfología de las partículas abrasivas e identificar los mecanismos de desgaste. Las tasas de erosión mostraron que el acero AISI S1 presentó mayor resistencia a la erosión que el acero AISI H13 tras el impacto constante de las partículas abrasivas. Además, las partículas de SiC causaron mayor daño por erosión en las superficies que las partículas de  $\text{Al}_2\text{O}_3$ .

**Palabras clave:** desgaste erosivo, acero AISI S1, AISI H13, forma de las partículas, tasas de erosión.

## I. INTRODUCTION

Erosive wear is one of the most damaging wear processes affecting mechanical components in industry; it accounts for approximately 70% of problems with mechanical components subjected to various damaging conditions. Essentially, it refers to the progressive loss of material due to the impact of abrasive particles or liquids on a surface. This type of wear commonly occurs in mold boxes and cores in die castings, pipes carrying liquids or gases, pipe fittings such as elbows, T-fittings, valves, chutes used in grain sorting machines (rice, corn, chickpeas, coffee), turbine blades, helicopter propellers, automotive paints or coatings, and other mechanical components. Due to this wear process occurs in different mechanical elements and materials, several erosion research studies have been conducted to determine the resistance of different types of steel alloys. For instance, Bingyuan Hong, et al. [1] conducted a study, in which the main objective was to experimentally investigate the erosion phenomenon of two very common materials used in pipelines for shale gas extraction, specifically AISI 304 stainless steel and L245 carbon steel, when impacted by solid particles entrained in gas. The author and his team discovered how factors such as gas velocity, impact angle, erosion time, and particle type affect wear. Additionally, analyses were performed using SEM to observe the metal surface after erosion and to understand the wear mechanisms. These experiments led to the discovery that the most critical impact angle for both materials was not the conventional  $90^\circ$ , but rather close to  $30^\circ$ , a condition in which particles behave like micro-blades, causing grooves and scratches on the surface. In contrast, at angles close to  $90^\circ$ , repeated impact favors the formation of cavities or craters. Furthermore, gas velocity was found to be an important parameter because it influences damage exponentially: the higher the velocity, the more severe the erosion. Regarding materials resistance, L245 carbon steel, being less hard, suffered significantly greater deterioration than 304 stainless steel. The explanation of the identified wear mechanisms was relevant because it explained why L245 carbon steel, having lower hardness, exhibited deeper grooves and larger craters compared to 304 stainless steel, thus supporting the differences observed in experimental erosion. In the context of foundry operations, where tool steels are constantly attacked by solid particles (silica sand particles), the phenomenon of erosive wear represents a significant threat for tools. Rodríguez, et al. [2] addressed this problem by investigating the erosive behaviour of two widely used steels: AISI H13 and AISI 4140. Their research demonstrates concisely that increasing material hardness through heat treatment is not entirely guaranteed to improve erosion resistance. In fact, for high impact angles (close to  $90^\circ$ ), harder steels suffered significantly greater material loss due to the formation of adiabatic shear bands, which act as sites for crack initiation and propagation. In this work, three clearly distinct wear regimes were identified. At low angles ( $10^\circ$  and  $20^\circ$ ), erosion tends to decrease as hardness increases, with micro-cutting being the predominant mechanism. In this case, particles act as small cutting tools that remove material and generate finer grooves in harder steels. In the range of  $30^\circ$  to  $40^\circ$ , the erosion rate remains practically constant without a clear dependence on hardness. For angles above  $60^\circ$ , softer materials show better erosion resistance than harder ones. In the latter, normal impact ( $90^\circ$ ) promotes crater formation and, furthermore, the appearance of shear bands that give rise to subsurface cracks, which considerably increases material loss.

Due to the interesting works mentioned above, interest arises in carrying out erosive wear tests on materials that are commonly used in mechanical elements such as mold boxes and cores in die castings. In this work, two alloy steels were subjected to erosion tests to know their behaviour against this wear process. Total erosion rates were obtained for both materials using two different particle shapes. The results showed significant differences in erosion damage.

## II. EXPERIMENTAL DETAILS

### A. Test procedure

The materials used in the tests were AISI S1 and AISI H13 steels (as-received condition), which are used to protect surfaces subjected to high fatigue and wear. Both materials were supplied in the form of standard steel slabs (25mm

wide and 3mm thick) and then cut carefully with a hacksaw crosswise to achieve the following dimensions, 50 mm X 25 mm and 3 mm in thickness to fix in the sample holder of the erosion rig. Additionally, hardness tests were conducted using a Microhardness Tester LECO LM 700. Five hardness data were calculated for each tested material in accordance to ASTM E384-17 [3] and an average value was obtained. The hardness of AISI S1 and AISI H13 steels was 320 HV and 363 HV, respectively. The applied load to the Vicker's indenter (square-based diamond pyramid) was 1000 gf, whereas the dwell time was 15 sec. In respect to the selected erodents, spherical  $\text{Al}_2\text{O}_3$  and angular SiC particles were employed to cause the erosion damage on the material surfaces. The morphology of both abrasives was obtained using a Radical 1200 model microscope and are shown in Fig. 1a-b.

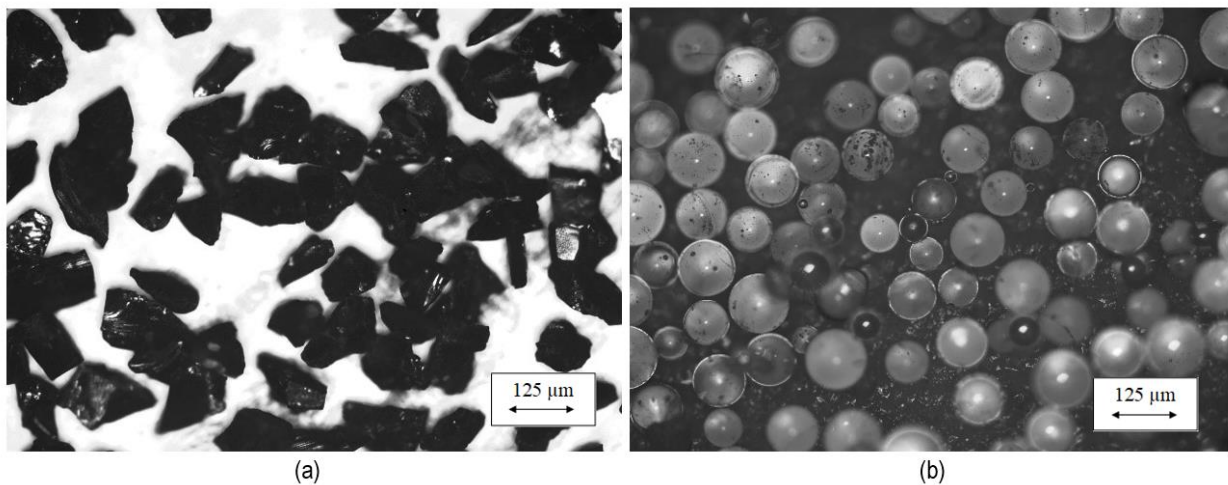


Fig. 1. Micrograph of abrasive particles, (a) Silicon carbide (SiC), (b) Alumina ( $\text{Al}_2\text{O}_3$ ).

The erosion tests were performed using a sand blasting erosion equipment, based on ASTM G76-95 [4]. The materials were subjected to erosion impacts by 10 min, however each sample was removed every 2 min to determine the mass loss. The impact angles were  $30^\circ$ ,  $45^\circ$ ,  $60^\circ$  and  $90^\circ$ . In addition, a particle velocity of  $30 \pm 2$  m/s and a particle flux of 63 g/min was used. In all tests, the samples were located 10 mm from the end of the stainless steel nozzle. The nozzle dimensions were 4.7 mm internal diameter, 6.3 mm external diameter and 260 mm length. The room temperature was between  $35^\circ\text{C}$  and  $40^\circ\text{C}$ . The specimens were weighed using an analytical balance (with an accuracy of  $\pm 0.0001$  g) before the start of each test (initial weight) and removed every 2 min, cleaned by using acetone and weighed again to measure the mass loss values. The micrographs of the eroded surfaces were analyzed using optical microscopy to identify the wear mechanisms of both steels at all incident angles.

### III. RESULTS

#### A. Wear mechanisms analysis

The micrographs of the erosion damage caused by SiC angular particles on AISI S1, are shown in Fig. 2a-b. Here, it is possible to observe typical wear mechanisms such as micro-cutting actions, irregular indentations (scratches), a few pits (small holes) and micro-ploughing actions on the worn surfaces at  $30^\circ$ . It is assumed that at lower impact angles ( $\alpha \leq 45^\circ$ ), the particles firstly impact the surfaces, causing a micro-cutting actions similar to that of a cutting tool, where material removal is significant [5], [6], [7], [8], [9]. Then, after this initial impact, some erosive particles slide

across the surface in various areas with such force that they cause wear similar to the ploughing action of the soil. In this particular case, the material is only removed or displaced due to the sliding of the particles. Irregular lines can also be caused by this action. In addition, more pits filled by wear debris, craters (large holes) and irregular indentations located in random areas, are seen on the damaged surfaces at 90°. These wear mechanisms are quite common at this incidence angle, because the abrasive particles act more directly on the surfaces.

On the other hand, the wear damage on AISI S1 inflicted by the impact of spherical alumina particles is shown in Fig. 2c-d. In this particular case, the material is more plastically deformed (displaced), and the pitting actions on the surface are consistent at 30°, whereas the erosion damage at 90° is characterized by craters seen on the surface of the AISI S1 steel and some pitting actions are identified as well. These wear mechanisms are very common when spherical particles impact the surfaces of different materials [10], [11], [12]. Due to the spherical shape of the particles, the wear intensity is lower compared to angular particles.

In relation to the wear damage on AISI H13 caused by SiC particles, the wear mechanisms were characterized by micro-cutting and micro-ploughing actions and scratches as observed in Fig. 3a-b. These mechanisms were also exhibited in other erosion studies using the same material [2]. On the other hand, the erosion damage originated by alumina impacts, is mainly characterized by large craters of different dimensions on the surfaces at 30° and a more uniform pitting action (small holes) are seen on the surfaces at 90°. In this specific case, the spherical particles actually left their shape printed on the surfaces of this material. Again, it is possible to see the differences in the mode of erosion damage caused by each of the particle shapes used in this work.

5

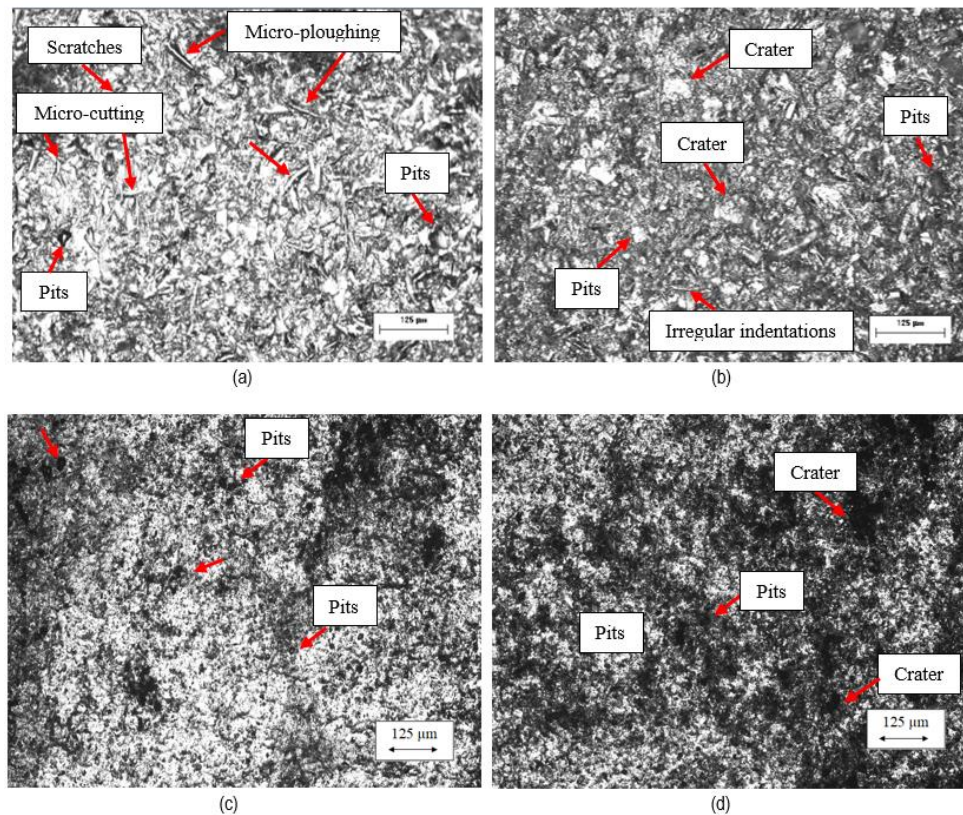


Fig. 2. Erosive wear on AISI S1 steel, (a) 30° SiC, (b) 90° SiC, (c) 30° Al<sub>2</sub>O<sub>3</sub>, (d) 90° Al<sub>2</sub>O<sub>3</sub>.

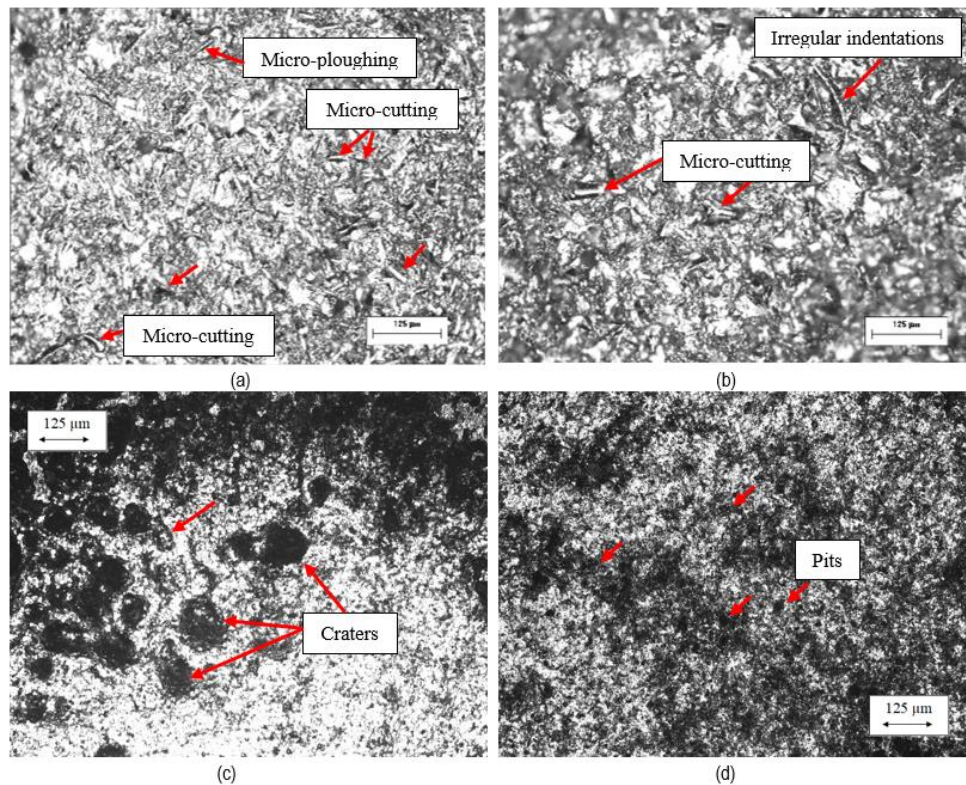


Fig. 3. Erosive wear on AISI H13 steel, (a) 30° SiC, (b) 90° SiC, (c) 30° Al<sub>2</sub>O<sub>3</sub>, (d) 90° Al<sub>2</sub>O<sub>3</sub>.

6

### B. Wear mass loss and erosion rates

Fig. 4a-d shows the mass loss vs time graphs of the tested materials at all incident angles. The curves showed a tendency to increase the damage over time. This trend has been commonly seen in other erosion studies [13]. The graphs show that silicon carbide caused significantly greater mass loss in each of the test materials compared to the results obtained using alumina. This was mainly due to the angular shape of the particles, which led to the removal of greater amounts of material from the steels due to the more severe micro-cutting actions. In the specific case of damage caused by silicon carbide, the performance of both steels was very close, which is related to the similarity of the wear mechanisms observed in both materials. In respect to mass losses caused by alumina, the behaviour of the materials was not as similar, and it was clearly observed that AISI S1 steel showed higher erosion resistance than AISI H13 steel. In fact, in general terms, AISI S1 steel performed better against this wear process.

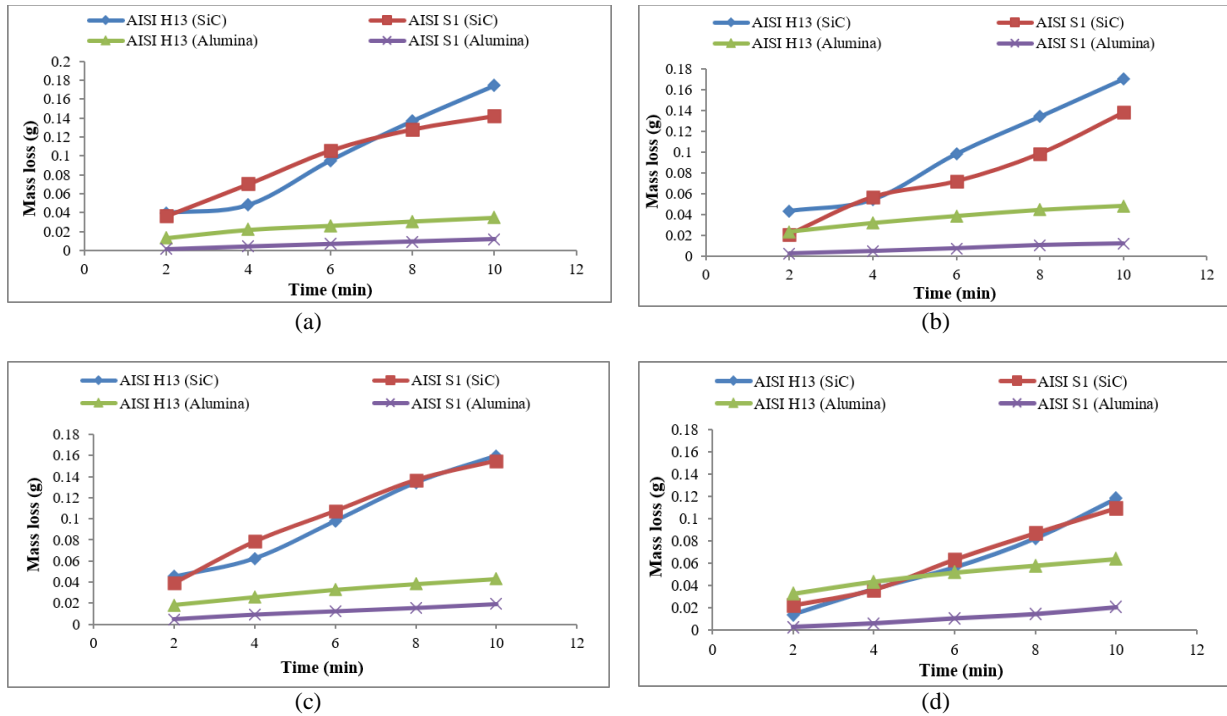


Fig. 4. Mass loss vs time graphs, (a) 30°, (b) 45°, (c) 60°, (d) 90°.

In respect to the erosion rates results, it is important to mention that the literature related to solid particle erosion indicates that materials exhibit ductile behaviour when they reach their maximum erosion rate at low impact angles ( $\alpha \leq 45^\circ$ ), while they present brittle behaviour when erosion rates are greater at higher angles, close to normal incidence ( $\alpha > 45^\circ$ ) [14]. Based on the literature, AISI H13 steel displayed ductile behaviour when impacted by silicon carbide at 30°, due to the constant and more intense micro-cutting actions of the angular particles. In contrast, when attacked with alumina particles, its behaviour was brittle, reaching its highest erosion rate at 90°. This could be because at 30°, the spherical particles regularly displace the material but do not detach it, while at 90°, these same particles can generate craters of considerable diameter, which can lead to higher erosion rates under normal conditions. On the other hand, AISI S1 steel exhibited similar brittle behaviour when impacted with both abrasive particles. The highest erosion rate was reached at 60° when impacted by silicon carbide, while the maximum erosion rate was observed at 90° as alumina was used for the erosion tests. In the case of silicon carbide, the combination of wear mechanisms such as micro-cutting, micro-ploughing, pitting, and craters may have been decisive in causing greater damage at this impact angle, while the alumina particles, based on the wear mechanisms observed, created a surface with a significant amount of pitting, which could have occasioned a high erosion rate at 90°.

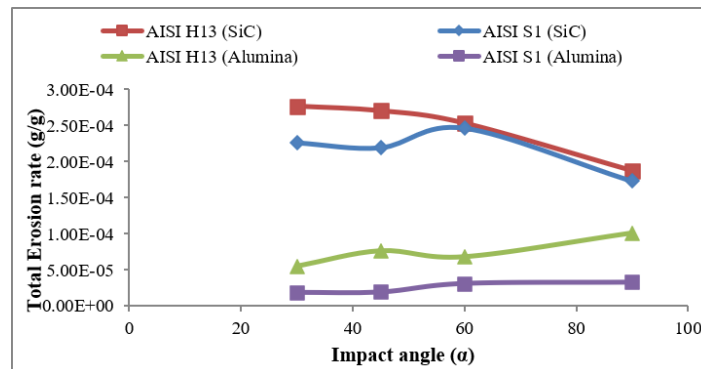


Fig. 5. Total erosion rates vs impact angles.

## IV. CONCLUSIONS

The results presented in this research work lead to the following conclusions,

1. In respect to the performance of both materials, it is possible to determine that AISI S1 exhibited higher erosion resistance than AISI H13 at all incidence angles and in each particle shape.
2. Erosion rates were much higher when angular silicon carbide was used for erosion testing compared to those obtained using alumina.
3. Typical wear mechanisms of solid particle erosion were identified; micro-cutting and micro-ploughing actions were observed due to the contact of angular particles on the surfaces of both materials. Furthermore, the formation of craters and holes or pits on the surfaces was common when spherical particles impacted both steels.

### CRedit (Contributor Roles Taxonomy)

**Author Contributions:** Conceptualization: JRLC; Methodology: JRLC; Investigation: ASCL, VVM; Writing-original draft preparation: JCS, HDLC; Writing-review and editing: JCS, HDLC; Supervision: JRLC; Formal analysis: ASCL, VVM.

**Funding:** This research received no external funding.

**Data Availability Statement:** The original contributions presented in this study are included in the article. Further inquiries can be directed to the corresponding author.

**Acknowledgments:** We recognize the experimental support of the Mechanical Laboratory of the Faculty of Mechanical and Electrical Engineering of the Universidad Veracruzana in Poza Rica and the Tribology Group of the SEPI-ESIME del Instituto Politécnico Nacional.

**Conflicts of Interest:** The authors declare no conflicts of interest.

## REFERENCIAS

- [1] B. Hong, Y. Li, X. Li, G. Li, A. Huang, S. Ji, W. Li, J. Gong, J. Guo, "Experimental investigation of erosion rate for gas-solid two-phase flow in 304 stainless steel/L245 carbon steel," *Petroleum Science*, vol. 19, pp. 1347-1360, Jan. 2022, doi: <https://doi.org/10.1016/j.petsci.2022.01.011>
- [2] E. Rodríguez, M. Flores, A. Pérez, R.D. Mercado-Solis, R. González, J. Rodríguez, S. Valtierra, "Erosive wear by silica sand on AISI H13 and 4140 steels," *Wear*, vol. 267, pp. 2109-2115, Aug. 2009, doi: <https://doi.org/10.1016/j.wear.2009.08.009>
- [3] American Society for Testing and Materials, *Standard Test Method for Microindentation Hardness of Materials*, ASTM E384, Am. Soc. for Testing and Materials, USA, 2017.
- [4] American Society for Testing and Materials, *Standard Test Method for Conducting Erosion Tests by Solid Particle Impingement Using Gas Jets*, ASTM G76, Am. Soc. for Testing and Materials, USA, 1995.
- [5] T. Deng, "Erosive Wear Mechanisms of Materials—A Review of Understanding and Progresses," *Materials*, vol. 18, pp. 1-28, April 2025, doi: <https://doi.org/10.3390/ma18071615>
- [6] A. K. Chauhan, D. B. Goel, S. Prakash, "Solid particle erosion behaviour of 13Cr–4Ni and 21Cr–4Ni–N steels," *Journal of Alloys and Compounds*, vol. 467, no. 1-2, pp. 459-464, Jan. 2009, doi: <https://doi.org/10.1016/j.jallcom.2007.12.053>
- [7] Md. A. Islam, T. Alam, Z. Farhat, "Construction of erosion mechanism maps for pipeline steels," *Tribology International*, vol. 102, pp. 161-173, Oct. 2016, doi: <https://doi.org/10.1016/j.triboint.2016.05.033>
- [8] Md. A. Islam, T. Alam, Z. N. Farhat, A. Mohamed, A. Alfantazi, "Effect of microstructure on the erosion behavior of carbon steel," *Wear*, vol. 332-333, pp. 1080-1089, May–June 2015, doi: <https://doi.org/10.1016/j.wear.2014.12.004>
- [9] P. Singh, P. Kumar, R. L. Viridi, "Investigation of solid particle erosion behaviour of SS-304 under different conditions," *Materials Today: Proceedings*, vol. 48, no. 5 pp. 1147-1152, Aug. 2021, doi: <https://doi.org/10.1016/j.matpr.2021.07.512>
- [10] Si-Qi Yang, Jian-Chun Fan, Ming-Tao Liu, De-Ning Li, Jun-Liang Li, Li-Hong Han, Jian-Jun Wang, Shang-Yu Yang, Si-Wei Dai, Lai-Bin Zhang, "Research on the solid particle erosion wear of pipe steel for hydraulic fracturing based on experiments and numerical simulations," *Petroleum Science*, vol. 21, pp. 2779-2792, Mar. 2024, doi: <https://doi.org/10.1016/j.petsci.2024.03.019>
- [11] T. Deng, M.S. Bingley, M.S.A. Bradley, "The influence of particle rotation on the solid particle erosion rate of metals," *Wear*, vol. 256, no. 11-12, pp. 1037-1049, Jun. 2004, doi: [https://doi.org/10.1016/S0043-1648\(03\)00536-2](https://doi.org/10.1016/S0043-1648(03)00536-2)
- [12] M. Hutchings, R. E. Winter, J. E. Field, "Solid particle erosion of metals: the removal of surface material by spherical projectiles," *Proceedings of the Royal Society of London. A.*, vol. 348, no. 1654, pp. 379-392, Mar. 1976, doi: <https://doi.org/10.1098/rspa.1976.0044>
- [13] Tkhabisimov, A. Mednikov, O. Zilova, "Studies of the Solid Particle Erosion Resistance of 30 L Steel with Different Types of Surface Modification," *Metals*, vol. 13, no. 12, pp. 1-17, Dec. 2023, doi: <https://doi.org/10.3390/met13121978>
- [14] M. Hutchings, P. Shipway, *Wear by hard particles. In Tribology: Friction and Wear of Engineering Materials*, 1st ed. London, UK: Edward Arnold, 1992.